Piezo-phototronic Effect Enhanced Perovskite Solar Cell Based on P(VDF-TrFE)

Jiaheng Nie [1,2], Yaming Zhang [1], Minjiang Dan [1], Jizheng Wang [2,*], Lijie Li [3,*], and Yan Zhang [1,*]

[1] *School of Physics, University of Electronic Science and Technology of China, Chengdu 610054, China*

[2] *Chinese Acad Sci, Inst Chem, Beijing Natl Lab Mol Sci, CAS Key Lab Organ Solids, Beijing 100190, China.*

[3] *College of Engineering, Swansea University, Swansea, SA1 8EN, UK*

[*] To whom correspondence should be addressed, E-mail: zhangyan@uestc.edu.cn, L.Li@swansea.ac.uk and jizheng@iccas.ac.cn

Abstract

As a candidate for next-generation solar devices, perovskite solar cells are increasingly being studied for their rapid increased power conversion efficiency (PCE). One of possible routes to further increase PCE has been the introduction of polarization in the absorption layer, which functions as a method for increasing built-in potential and reducing interface barrier, leading to much improved carrier separation and extraction. This technique uses the principle of the piezo-phototronic effect utilized for obtaining enhanced optoelectronic performances. In order to introduce internal polarization while maintaining optical absorption performance of the perovskite, an organic-inorganic hybrid perovskite composite film solar cells have been fabricated by doping polarized Polyvinylidenefluoride-co-Trifluoroethylene (P(VDF-TrFE)) into the perovskite in this work. The composite film has been polarized with an external potential, subsequently inducing the piezo-phototronic effect to enhance the performances of perovskite solar cells. Experimental results show that this simple polarization method has effectively improved several key characteristics of the solar cell. The power conversion

This article has been accepted for publication and undergone full peer review but has not been through the copyediting, typesetting, pagination and proofreading process, which may lead to differences between this version and the Version of Record. Please cite this article as doi: 10.1002/solr.202100692

efficiency has reached up to 22.1%, short circuit current (J_{sc}) increases to 24.2 mA/cm^2, and open circuit voltage (V_{oc}) increases to 1.18 V.

Keywords: piezo-phototronics, perovskite, P(VDF-TrFE), polarization, power conversion efficiency (PCE)

1. Introduction

The cutting-edge research of perovskite solar cell (PSC) showed that the power conversion efficiency of perovskite solar cell (PSC) has been achieved to around 25%, due to high carrier mobility and light response of these materials.[1] For example, solar cells based on organic-inorganic lead halide perovskite (ABX_3, A=MA (CH_3NH_3) or FA ($CH(NH_2)_2$), B=Pb or Sn, X= Cl, Br, or I) have great advantages of high photoluminescence (PL) quantum efficiency, and superior photoelectric conversion property.[2] Although various approaches have been developed to improve cell efficiency, such as compositional engineering,[3] interface engineering,[4] and solvent engineering,[5] the purpose of these strategies is to reduce fundamental energy losses by improving the separation of carriers,[6] and enhancing carrier extraction at the interface. As for separation of carriers, the separation and drifting process of electrons and holes are strongly affected by built-in field (BIF). The polarization can increase BIF and improve carrier separation process.[7, 8] As for the carrier extraction at interface, the interface dipoles formed by polarization on the surface match the effective work function.[9] The permanent and strong dipoles of polymers can enhance the injection of electrons.[10] The injection efficiency of carriers were modulated by the interface effects including energy level alignment and Schottky barrier in the multi-layer structure.[11] Polyelectrolytes were fabricated as the hole transportation layer and were well matched to the energy bands of perovskite, leading to high level of promoting hole transport from the light absorbing layer to the ITO anode layer.[12]

The polarization can modulate the separation, recombination, and transport process of carriers,[13] named as piezo-phototronics effect. This new principle has produced a unique mechanism used to enhance devices efficiency,[14] which has shown great potential in various devices and systems such as nanogenerators, energy harvesting systems, and a series of optoelectronic devices for photoelectric sensing, strain mapping, and optical-communication systems.[15] It has been reported that CsPbBr3@PVDF composite fibers using excellent piezoelectric properties of PVDF, realized the long-term stability of the inorganic lead halide perovskite, revealed a high open-circuit voltage (V_{oc}) of 103 V and short-circuit current of 170 μA/cm^2.[16] A flexible composite film based on P(VDF-TrFE)/CsPbBr3 quantum dots

illustrated much enhancement in output performance with V_{oc} of 11.5 V under 0.6 MPa, and piezoelectric coefficient of 24.5 pC/N. [17] Based on prominent piezoelectric response and photoresponse, PVDF-doped perovskite film also can be a self-powered photoactive piezoelectric energy harvester.[18] Composed of lead halide perovskite and PVDF, a high-performance piezoelectric nanogenerators has been reported to drive the commercial light-emitting diode (LED).[19] A fundamental study has demonstrated the mechanism of piezo-phototronics affecting electrons or holes transport separately.[20] A group of high performance piezo-phototronic devices have been developed, such as nanowires (NWs) array,[21] two-dimensional nanomaterial devices,[22] solar cells,[23] photodetectors,[24] and light-emitting diodes (LED).[25] Perovskite and PVDF based composite films owning the mechanical energy-harvesting and light response properties, have been reported to be a self-powered flexible photoactive piezoelectric energy harvester in piezo-phototronic technology, exhibit fast response time of 44 ms (rising time) and 153 ms (decaying time) and the wavelength range of about 460 nm ~ 630 nm.[26] Cao et al. integrated P(VDF-TrFE)-perovskite bulk heterojunction film photodetector, displaying the ultrahigh performance with detectivity of 1.4×10^{13} Jones and response time (92/193 μs) in the wavelength of 650 nm.[27] Subsequently, they fabricated P (VDF - TrFE)-assisted perovskite nanowire arrays, illustrated an ultrahigh detectivity of 7.3×10^{12} Jones and the response time of 88/154 μs with the detecting wavelength range of about 300-800 nm.[28] Due to introduction of these polymers, these fabricated photodetectors based on P(VDF-TrFE) and perovskite show excellent performance in self-powered and photoresponse properties. These demonstrate a huge potential for piezo-phototronic photodetector devices. Due to the high sensitivity upon environmental stimuli, flexible optoelectronic devices were also achieved to mimic human visual and tactile systems.[29]

The carrier separation and extraction are two distinct processes. The enhancement of BIF and improvement of interface matching are generally accomplished by different and separated layers. Here, we introduce a simple polarization process that directly enhance the built-in electric field and the improved interface matching into one process. The polarization of P(VDF-TrFE) increases the built-in electronic field, which greatly promotes the carrier separation. The charges induced by P(VDF-TrFE) at the surface of perovskite# P(VDF-TrFE)

composite films can control the surface potential of films and the charges distribution of absorption layer and carrier transport layer for reducing the interface barrier. Therefore, the photovoltaic properties of doped P(VDF-TrFE) perovskite solar cell have been enhanced by the polarization process based on the piezo-phototronic effect.

An organic-inorganic hybrid perovskite solar cell was fabricated based on the perovskite-P(VDF-TrFE) piezoelectric composite thin film. The schematic of spontaneous polarization, the perovskite solar cell device structure and device pre-polarization process are illustrated in Figure 1. The device is fabricated by an n-i-p sandwich structure of the electron-transporting layer (SnO_2), the photoactive perovskite layer ($(FAPbI3)_{1-x}(MAPbBr_{3-y}Cl_y)_x$), and the hole-transporting layer (2, 2′ , 7, 7′ -Tetrakis -[N, N -di(4 -methoxyphenyl) amino] -9, 9' -spiro -bifluorene, (Spiro-OMeTAD)). Figure 1a shows the spontaneous polarization state of device, directly after the preparation. By adjusting the polarization orientation through the external positive or negative bias voltage, the efficiency of solar cells demonstrates increasing or decreasing trends. Figure 1b shows the polarization process with the 2 V/μm external bias voltage. Figure 1c shows that the polarized P(VDF-TrFE) induced electronic field affects transport behavior of electrons and holes. After the polarization, there is a strong local electric field effect near the dipole of P(VDF-TrFE) in perovskite composite film. Local carrier transport process affected by the local field is shown in Figure 1d. Incorporated P(VDF-TrFE) polymer produces a local electric field, widens the depletion, and results in a strong local built-in field. Figures 1e and 1f illustrate the molecule structure of perovskite and P(VDF-TrFE).

The PCE of fabricated solar cell devices increases from 18.3% to 22.1%. Recordable J_{sc} has increased to 24.2 mA/cm^2 at the 2.50 mg/mL concentration of P(VDF-TrFE) compared to 21.9 mA/cm^2 for the perovskites without P(VDF-TrFE), indicating that doped P(VDF-TrFE) polymer can enhance photovoltaic properties. Fill Factor and V_{oc} have been achieved to 78% and 1.18 V respectively. The surface polarization state of doped composite film was studied by Kelvin probe force microscopy (KPFM). The spontaneous polarization of the polymer promotes the charge polarization of the perovskite film. Bases on piezo-phototronic effects, this work provides an effective and novel approach to improve the performances of optoelectronic devices and perovskite solar cells, and these results exhibit a great prospect of piezoelectric

polymer enhancing photovoltaic characteristics of organic-inorganic lead halide perovskite materials in future high-performance piezo-phototronic and piezotronic multifunctional devices.

2. Carrier collection improvement in a simple polarization process

P(VDF-TrFE) doped perovskite solar cell devices have been fabricated by the sequential deposition method. A mixed solution of perovskite and P(VDF-TrFE) was stirred at a temperature of 60 °C for eight hours on a stirring table for thorough mixing. The SnO_2 solution, precursor fluid, and Spiro-OMeTAD are sequentially deposited onto the ITO-coated glass substrate by spin coating and annealing process. The uniform composite films based on perovskite and P(VDF-TrFE) form a black light-absorbing layer.

The doping effect of P(VDF-TrFE) polymers on the organic-inorganic hybrid perovskite solar cell was investigated by scanning electron microscopy (SEM). Figures 2a and 2b show the top-view morphology images of P(VDF-TrFE)-modified (2 mg/mL) perovskite films and untreated perovskite films, respectively. The surface morphology of P(VDF-TrFE)/perovskite composite films with bigger grain sizes than the untreated film. Figure 2c shows the statistics of size scale with perovskite and P(VDF-TrFE)/perovskite films. Through doping improved morphology, these composite films based on the piezoelectric material enhance the organic photovoltaic properties. Figure S1 shows the cross-section morphology of fabricated solar cells based on doped P(VDF-TrFE) polymer with the sandwich structure of treated perovskite composite films. Figure S2 illustrates the absorption spectrum of P(VDF-TrFE) polymer doped perovskite composite films which demonstrates increased light absorption in the range of the visible spectrum. P(VDF-TrFE) films are very poor light absorbent material. However, the light absorption of the perovskite after the addition of P(VDF-TrFE) has been improved. The increase of absorption characteristics were considered from the dielectric constant optimization due to the P(VDF-TrFE) doping perovskite colloidal compounds.[30] The steady-state Photoluminescence (PL) spectrum of the perovskite films based on various concentrations of P(VDF-TrFE) polymers are shown in Figure 2d. For perovskite composite films, a PL peak was around 770-780 nm and appear slight red shift with the increase of P(VDF-TrFE) doped content. The doped 2 mg/mL P(VDF-TrFE)/perovskite composite films illustrate a strong PL intensity,

indicating this concentration composite film has the lowest carriers' recombination. The doped P(VDF-TrFE) polymer of excessive concentration destroys the structure of perovskite, resulting in a decrease in light absorption efficiency.

XRD profiles demonstrate the effect of various concentrations of P(VDF-TrFE) on the film development process, as shown in Figure 2e. Perovskites with different P(VDF-TrFE) have similar diffraction peaks at the same positions (14.16°, 24.56°, 28.40° marked by an asterisk.). The current view indicates that excess PbI_2 at grain boundary can effectively passivate surface defects of perovskite and increase the V_{oc} of perovskites.[30] P(VDF-TrFE) was reported that β-phase has a peak near 19° .[31] The changes of doping different P(VDF-TrFE) in the crystallization process are obtained by the relative peak intensity change of PbI_2 (at 12.8°, marked as #) and perovskite. The intensity of perovskite peaks achieves the maximum value at P(VDF-TrFE) concentration of 2 mg/mL. Aggregated polymer particles will hinder perovskite crystallization, resulting in a peak value of PbI2 higher than adjacent perovskite. The perovskites have randomly orientated characteristic due to its spontaneous polarization. The disorder of spontaneous polarization may lead to higher carrier recombination and affect the drift speed of carriers. It is revealed that local electric potential caused by dipoles provide a local microscopic separating field for electron-hole pairs, and accelerate the exciting dissociate.[32] The orientation consistency of the dipole and strong local electric field may be the effective methods to promote carrier's production efficiency. Simultaneously, doped fluorination promotes lower exciton binding energy, which affects the important carriers generation and recombination.[33] Figure 2f shows I-V curves of perovskite solar cell devices with various concentration of P(VDF-TrFE). As shown in Table 1, the V_{oc} of 0 mg, 1 mg, 2 mg, and 4 mg are 1.14 V, 1.16 V, 1.16 V, and 1.18 V. The J_{sc} of 0 mg, 1 mg, 2 mg, and 4 mg are 21.9 mA/cm^2, 22.9 mA/cm^2, 23.6 mA/cm^2, and 22.9 mA/cm^2. The FF of 0 mg, 1 mg, 2 mg, and 4 mg are 72.8%, 72.9%, 72.1%, and 69.0%. The corresponding PCE are 18.3%, 19.2%, 20.3%, and 18.8%. J_m or V_m is the value of the current density and voltage at the maximum power point of curve. The slope of J-V curve is determined by the $1/R_{sh} = dJ/dV$, at the $V < V_m$, and R_{sh} is the shunt resistance. According to the model of organic solar cells, this part of *J-V* curve should be horizontal, that is, the slope is zero, $R_{sh} = \infty$, at the $V < V_m$. When $V > V_m$,[34] the scope of *J-V*

curve is determined by the $1/R_s = dJ/dV$, where R_s is series resistance. This part of *J-V* curve should be vertical, that is R_s = 0 in the ideal condition. Compared to the curve of the 2 mg P(VDF-TrFE) doped concentration, the R_{sh} has no significant change and R_s increases, at the curve of the 2 mg P(VDF-TrFE) doped concentration. R_s is mainly caused by the resistivity of the perovskite layer, indicating that excessive PVDF concentration leads to higher resistance. Chiang et al. thought that J_{sc} is affected by conductivity, carrier mobility and diffusion length of the active layer.[35] The rising resistance reduces FF, and does not affect V_{oc}.[36] Kim et al. improved the fill factors of lead-halide perovskite solar cells, by decreasing the series resistance.[37] The lower R_s (higher conductivity) the better carrier transportation efficiency, which mainly leads to the better J_{sc} and FF. In our experiments, the excessive PVDF concentration greatly impedes the carriers transport process, by increasing the resistance of perovskite and interface barrier at the junction. Hence, J_{sc} of device decreases. The trends of J_{sc}, FF and PCE show that doped P(VDF-TrFE) polymers enhance the device performances by reducing the surface defects. In the solar cell with micro-nano structures, the interfacial properties dominate the transport characteristics and improve interface binding.[38] Figure S3 illustrates the x-ray photoelectron spectra (XPS) data of perovskite films treated with 0 mg, 1 mg, 2 mg, 4 mg P(VDF-TrFE). The surface compositions are determined by these spectra, and the concentration of elemental species is quantitatively estimated by the spectroscopic intensities. As shown in Figure S3a, the elements of C, N, Pb, I, F, belonging to the perovskite and P(VDF-TrFE) polymer were found in the P(VDE-TrFE)/perovskite films. For C, N, Pb, I, F elements, The XPS spectra of the F-1s (Figure S3b), Pb-4f (Figure S3c), C-1s (Figure S3d), I-3d (Figure S3e), N-1s (Figure S3f) illustrate the peak shifting to higher binding energy. This may indicate polarization induced electron transfer of elements.

Figure 3 shows the I-V curves of 2 mg P(VDF-TrFE) doped perovskite solar cell after positive or negative polarization. The excessive bias voltage may damage the solar cell devices, experimentally. These devices were fabricated using two-step methods, which have high power conversion efficiencies.[39] Figure 3a displays the energy conversion performance after positive polarization of 0 min, 10 min, 20 min, and 40 min. J_{sc} increases from 23.6 mA/cm^2 to 24.2 mA/cm^2, and FF increases from 72.1% to 78.0%. The PCE finally achieves 22.1% that is higher

than 20.3% of the unpolarized device (full parameters after positive polarization are shown Table 2). It is clear that the efficiency improvement in the polymers doped perovskite solar cell is mainly derived from the significant increase of V_{oc} and FF. Figure 3b displays the energy conversion performance after negative polarization of 0 min, 10 min, 20 min, and 40 min. J_{sc}, V_{oc} and FF are 23.5 mA/cm^2, 21.7 mA/cm^2, 20.3 mA/cm^2, 20.2 mA/cm^2, 1.13 V, 1.12 V, 1.14 V, 1.09 V, 77%, 75%, 72.7%, 64% respectively. After 40 min polarization, the PCE decreases from 20.5% to 14.3%. The device characteristics after negative poling are shown in Table 3. These experiments conclude that the unique coupling effect between piezoelectric and semiconductor properties further improves the performances of solar cell devices.

3. Piezo-phototronic effect on perovskite solar cell

Perovskite crystalline has a tetragonal perovskite crystal structure, and the polarizable organic cation MA^+ is in 12-fold cuboctahedral coordination.[40] The low bulk-charge separation efficiency hinders the high performance of photovoltaic devices, and an internal electric field is demonstrated to be an effective solution to this limitation.[41] P(VDF-TrFE) can further enhance the lattice polarization of perovskite due to its excellent polarization characteristics. For photovoltaic devices based on piezoelectric materials, its photovoltage is observed higher than the electric bandgap of material, by controlling the carriers near piezoelectric domain walls in nanoscale methods.[42] It is reported that tailoring the structure and lattice strain of crystal induces the enhanced electric field, promotes an over 7.5 times larger photocurrent.[43] A mixed-ligand-induced quantum-dot electric field also promotes the generation efficiency, improves the overall cell power conversion efficiency.[44] In inorganic piezoelectric photovoltaic devices, the large internal electric field induced by permanent electric polarization of piezoelectric polymer gives rise to an enhanced conversion efficiency.[7]

The built-in electric field of perovskite film doped by P(VDF-TrFE) is given by [7]

$$E = \frac{d\sigma_P}{\varepsilon_0 \varepsilon_{FE} L} \quad (1)$$

where σ_P is the polarization charge density, d is the thickness of the P(VDF-TrFE) layer, L is the thickness of the polymer semiconductor layer and ε_{FE} is the relative dielectric constant of

the P(VDF-TrFE)/perovskite composite film. Equation (1) shows that there is a direct proportional relationship between the built-in electric field and the polarization of the polymer. For the carrier management, in addition to enhancing the separation of the carrier, the built-in electric field induced by P(VDF-TrFE) polymer can be expected to improve the drift speed and drift length of carriers. Applying a reliable strong electric field becomes a mechanism for preventing the recombination of free carriers. Certainly, minimizing carrier recombination probability is related to the local electric field strength. Typically, a work function difference across the p-layer and n-layer produces a weak electric field. The polarized charges from polymer after pre-polarization provides over ten times higher intrinsic electric field intensity.[45] Galipeau et al. determined the 5.7 MV/m value of internal electric field of perovskite, using the combination of theory and experiment.[46] Taguchi et al. reported the built-in electric field intensity of about 1.2 MV/m in the organic solar cell, due to the photovoltaic effect.[47] Lee et al. reported that the value range of internal electric fields of p-i-n solar cell is about 3.8 ~ 4.4 MV/m.[48] Fu et al. reported an about 200 MV/m of average electric field in the PVDF/perovskite-based composites under the condition of spontaneous polarization.[49]

Figure 4 shows the schematic and band diagram for p-i-n solar cell under the positive or negative polarization effect. Figure 4a shows the energy band state in the condition of spontaneous polarization. P(VDF-TrFE) dipoles are scattered inside the perovskite film. Figure 4b illustrates the change of energy band under positive poling. Due the positive poling, the built-in electronic field is enhanced, energy band decreases, the V_{oc} increases. The dissociation efficiency of carriers depends on the magnitude of the local electronic field. The polarization electric field is much larger than the built-in electric field, leading to a higher separation efficiency of electron-hole pairs and a higher transportation efficiency of carriers. The carriers can enter the corresponding transport layer much more smoothly by decreasing interface barriers. Figure 4c shows the effect of negative polarization on energy bands. The negative polarization decreases the built-in electric field, enhancing the composite of electronic cavity pairs. It has been reported the doped P(VDF-TrFE) composite films have longer photoluminescence (PL) lifetime under positive polarization.[31] For positive polarization case, the curved band is offset upward, and polarized electric field enhances built-in electric field, promotes more carriers drift from active layers to p-layer or n-layer. The negative polarization

shows the opposite trend.

To investigate the impact of spontaneous polarization on work functions, and energy band of perovskite, ultraviolet photoelectron spectroscopy (UPS) measurements have been performed. As shown in Figure S4 (the E_{cutoff} values of perovskite are 16.93 eV, 16.92 eV, 16.75 eV, and 16.79 eV, respectively in spontaneous polarization of different concentration of P(VDF-TrFE). According to $W_f = h\nu - E_{cutoff}$, where hν=21.22 eV. The work functions of perovskite are 4.29 eV, 4.30 eV, 4.47 eV, 4.43 eV respectively, where the doped P(VDF-TrFE) concentrations are 0 mg, 1 mg, 2 mg, and 4 mg. Figure S 4c-4f show the valence band maximum (VBM) spectra, The VBM of perovskites in the doped P(VDF-TrFE) concentration of 0 mg, 1 mg, 2 mg, 4 mg are 1.85 eV, 1.82 eV, 1.76 eV, 1.80 eV respectively. Therefore, the valence bands of 0 mg, 1 mg, 2 mg, 4 mg P(VDF-TrFE) doped perovskite are 6.14 eV, 6.12 eV, 6.23 eV, and 6.23 eV respectively, according to the equation $E_v = W_f + E_{VBM}$. Thus, the spontaneous polarization of P(VDF-TrFE) changes the energy level of perovskite surface.

The change of surface potential induced by polarization of the P(VDF-TrFE)/perovskite piezoelectric composite thin films were measured by KPFM. Figure 5 shows the KPFM images of perovskite films of positive polarization. KPFM image of pristine perovskite film is shown in Figure 5a. Figures 5b, 5c and 5d show the surface potential based on perovskite doped by 1 mg, 2 mg, 4 mg P(VDF-TrFE). The darkening of the image indicates spontaneous polarization of doping P(VDF-TrFE) affects the polarization of perovskite films, which leads to decreased surface potential of films. The local surface potential difference of doped 0 mg, and 2 mg P(VDF-TrFE), as shown in Figure 5e. The overall potential distribution difference is shown in Figure 5f. The surface potential of perovskite film doped by P(VDF-TrFE) was 50 mV lower than the pristine film. Polarization of P(VDF-TrFE) affects the work function of surface.[50] The surface roughness and surface potential of KPFM is shown in Figure S5. The surface potential differences caused by different concentrations of P(VDF-TrFE) is shown in Figure S6. Figure S7 shows surface potential differences induced by the negative polarization. The doping concentration of P(VDF-TrFE) induced the surface potential difference, and the difference has reached up to 0.1 V, as shown in Figure S7 and S8. The surface topographies have no obvious change in perovskite film with different doped P(VDF-TrFE) polymer. The surface potential is

related to the work function. KPFM measurements have shown that surface potential further decreases after the positive poling process, which reveals that the polarized polymer does promote the polarization of the perovskite lattice. It is also reported that the contact potential difference across the interface measured by KPFM shows that V_{bi} in P(VDF-TrFE)/perovskite composite films is higher than perovskite films.[8] Figure S9 and S10 show the effect of irregular polarizations.

Piezo-phototronic is a concept that polarization charges can modulate the generation, separation, and transportation. P(VDF-TrFE) polymer is doped into a perovskite layer of solar cell devices, to generate polarization electric field and to improve optical parameters, leading to enhanced efficiency. The polarization of P(VDF-TrFE) polymer not only improve carrier separation, but also reduce the barrier and work function of the interface.[51] The ionic transport properties of polymers can be affected by external bias voltage, due to ion conductivity of polymers modulated by electronic field.[52] The energy level alignment and Schottky barrier bending in the interface region affects the generation and separation efficiency of photogenerated carriers.[53] Thus, the enhancement of photovoltaic properties stems from the modulation of the piezoelectric polarization charges induced by P(VDF-TrFE) inside the perovskite. Therefore, the open circuit voltage V_{oc}, the fill factor and short-circuit current improve by one polarization process.

5. Summary

To conclude, novel device prototypes making use of the principle of piezo-phototronics enhancing the performance of perovskite solar cells have been presented. The polarization has been introduced to enhance the performance of perovskite solar cells, by doping P(VDF-TrFE) into the perovskite layers. The simple poling process promotes the efficient separation and extraction for internal and interface carriers. The strong local electric field caused by polarization and the change of the interface barrier caused by the interface dipoles jointly regulate the transport behavior of internal carriers. The polarized dipoles of the film prevent the recombination of a considerable number of electrons and holes, driving carriers to drift to transport layers, increasing charge-collection efficiencies. The J_{sc}, V_{oc} and PCE have been achieved to 24.2 mA/cm^2 1.18 V, and 22.1% after polarization. Comprehensive theoretical and

experimental investigations manifest the convenience and efficiency of doping P(VDF-TrFE) polymers. Our work provides a novel and feasible method for further enhancing the efficiency of perovskite solar cells, and further expand the application of the piezotronics and piezo-phototronics in the perovskite solar cells and related energy conversion devices.

EXPERIMENTAL SECTION

Solution process: Electric transport layer (ETL) uses the diluted solution of the SnO_2 colloid precursor and ultrapure water with a ratio of 1.2:6.5. Firstly, PbI_2 solution was prepared by dissolving PbI_2 of 760 mg in 1.16 mL mixed solvent of (N, N-Dimethylformamide) DMF and DMSO with a ratio of 1:0.16. Then P(VDF-TrFE) powders are fully dissolved in PbI_2 precursor solution to form mixed solution with the concentrations of 0 mg/mL, 1 mg/mL, 2 mg/mL,5 mg/mL, respectively. Subsequently, All the solutions are placed on the stirring table at 60 ° C for 8 hours to ensure complete reaction. The mixed ammonium salt isopropanol solution is prepared by dissolving the 110 mg FAI, 11.5 mg MACl and 11 mg MABr in 1.5 mL isopropanol solvent. The spiro-OMeTAD precursor was dissolved spiro-OMeTAD of 72.3 mg in 1 mL chlorobenzene with 35 μL LiTFSI/acetonitrile mixed solution (520 mg LiTFSI in 1 mL acetonitrile) and 28.8 μl 4-tBP. After filtering, all solutions are prepared for fabricating perovskite solar cells.

Device Fabrication: After cleaned with ultrapure water, acetone, and isopropanol for 20 minutes respectively, these ITO-coated glass substrates (20 ± 5 ohms/sq) are treated by plasma cleaning devices. For the fabrication of the electric transport layer (ETL), SnO_2 solution is spun coated onto ITO-glass substrate at 3500 rpm for 35 s. After the annealing process at 150 ° C for 30 min, the sample was taken to the glove box for (P(VDF-TrFE))-perovskite films. Perovskite layer is fabricated by two-steps methods. Firstly, PbI_2 solutions with various concentrations of P(VDF-TrFE) are spin-coated onto the SnO_2 layer at 1600 rpm for 23 s and 4000 rpm for 27 s, then annealing at 70 ° C for 2 min. Secondly, the mixed ammonium salt isopropanol solution is deposited onto the PbI_2 layer by spin coating method at 2000 rpm for 23 s, then perovskite layer is annealed at 140 ° C for 20 min out of the glove box (40% relative humidity). Hole transport layer (HTL) was deposited onto perovskite layer by spin-coating method at 4000 rpm for 30 s. After 20 hours, ~70 nm Au electrode was deposited by vacuum

evaporation under the pressure of 2×10^{-4} Pa.

Characterization: The effective area for absorbing light of perovskite solar cell device is 0.04 mm^2. J–V curves were measured by using a computerized Keithley 2420 source meter and a Xenon-lamp-based solar simulator (Enli Tech, AM 1.5G, 100 mW/cm^2). The illumination intensity of the solar simulator was determined by using a monocrystalline silicon solar cell (Newport, Oriel Sol3A Class AAA, 94043A). We perform I-V tests of photodetector using the setup composed of Keithley 4200 and Micromanipulator 6150 probe station at room temperature and the ambient air pressure. The optical source is the white light from the Z-105WA Halogen lamp. Absorption spectra were quantified using the JASCO V-570 spectrophotometer. UPS and XPS data were measured by ESCALAB250XI, Thermo Fisher Scientific. The XRD patterns is studied by Rigaku-2500 X-ray diffractometer (CuKα radiation, λ =1.5406 Å). The SEM images were taken by the S-4800, Japan.

References

[1] Q. Lin, A. Armin, R. C. R. Nagiri, P. L. Burn, P. Meredith, Nature Photonics 2014, 9, 106; J. Tong, Z. Song, D. H. Kim, X. Chen, C. Chen, A. F. Palmstrom, P. F. Ndione, M. O. Reese, S. P. Dunfield, O. G. Reid, J. Liu, F. Zhang, S. P. Harvey, Z. Li, S. T. Christensen, G. Teeter, D. Zhao, M. M. Al-Jassim, M. van Hest, M. C. Beard, S. E. Shaheen, J. J. Berry, Y. Yan, K. Zhu, Science 2019, 364, 475; M. Jeong, I. W. Choi, E. M. Go, Y. Cho, M. Kim, B. Lee, S. Jeong, Y. Jo, H. W. Choi, J. Lee, J. H. Bae, S. K. Kwak, D. S. Kim, C. Yang, Science 2020, 369, 1615.

[2] P. Gao, M. Grätzel, M. K. Nazeeruddin, Energy Environ. Sci. 2014, 7, 2448; M. A. Green, A. Ho-Baillie, H. J. Snaith, Nature Photonics 2014, 8, 506; Z. L. Wang, T. Jiang, L. Xu, Nano Energy 2017, 39, 9.

[3] N. J. Jeon, J. H. Noh, W. S. Yang, Y. C. Kim, S. Ryu, J. Seo, S. I. Seok, Nature 2015, 517, 476.

[4] H. Zhou, Q. Chen, G. Li, S. Luo, T. B. Song, H. S. Duan, Z. Hong, J. You, Y. Liu, Y. Yang, Science 2014, 345, 542.

[5] N. J. Jeon, J. H. Noh, Y. C. Kim, W. S. Yang, S. Ryu, S. I. Seok, Nat Mater 2014, 13, 897.

[6] L. C. Hirst, N. J. Ekins-Daukes, Progress in Photovoltaics: Research and Applications 2011, 19, 286.

[7] Y. Yuan, T. J. Reece, P. Sharma, S. Poddar, S. Ducharme, A. Gruverman, Y. Yang, J. Huang, Nat Mater 2011, 10, 296.

[8] C. C. Zhang, Z. K. Wang, S. Yuan, R. Wang, M. Li, M. F. Jimoh, L. S. Liao, Y. Yang, Adv Mater 2019, 31, e1902222.

[9] H. Ishii, K. Sugiyama, E. Ito, K. Seki, Advanced Materials 1999, 11, 605; H. Wu, F. Huang,

J. Peng, Y. Cao, Organic Electronics 2005, 6, 118.

[10] Z. He, C. Zhong, S. Su, M. Xu, H. Wu, Y. Cao, Nature Photonics 2012, 6, 591.

[11] Y. Liu, J. Guo, E. Zhu, L. Liao, S. J. Lee, M. Ding, I. Shakir, V. Gambin, Y. Huang, X. Duan, Nature 2018, 557, 696.

[12] H. Choi, C. K. Mai, H. B. Kim, J. Jeong, S. Song, G. C. Bazan, J. Y. Kim, A. J. Heeger, Nat Commun 2015, 6, 7348.

[13] Z. L. Wang, W. Wu, National Science Review 2014, 1, 62; Y. Zhang, Y. Leng, M. Willatzen, B. Huang, MRS Bulletin 2018, 43, 928; J. Hao, C.-N. Xu, MRS Bulletin 2018, 43, 965.

[14] Z. L. Wang, Adv. Mater. 2012, 24, 4632.

[15] W. Wu, X. Wen, Z. L. Wang, Science 2013, 340, 952; W. Wu, L. Wang, Y. Li, F. Zhang, L. Lin, S. Niu, D. Chenet, X. Zhang, Y. Hao, T. F. Heinz, J. Hone, Z. L. Wang, Nature 2014, 514, 470; W. Wu, Z. L. Wang, Nature Reviews Materials 2016, 1.

[16] H. Chen, L. Zhou, Z. Fang, S. Wang, T. Yang, L. Zhu, X. Hou, H. Wang, Z. L. Wang, Advanced Functional Materials 2021, 31, 2011073.

[17] J. Nie, L. Zhu, W. Zhai, A. Berbille, L. Li, Z. L. Wang, ACS Applied Electronic Materials 2021, 3, 2136.

[18] S. Mondal, T. Paul, S. Maiti, B. K. Das, K. K. Chattopadhyay, Nano Energy 2020, 74, 104870.

[19] R. Ding, X. Zhang, G. Chen, H. Wang, R. Kishor, J. Xiao, F. Gao, K. Zeng, X. Chen, X. W. Sun, Nano Energy 2017, 37, 126.

[20] H. Zou, X. Li, W. Peng, W. Wu, R. Yu, C. Wu, W. Ding, F. Hu, R. Liu, Y. Zi, Z. L. Wang,

Adv Mater 2017, 29.

[21] C. Pan, L. Dong, G. Zhu, S. Niu, R. Yu, Q. Yang, Y. Liu, Z. L. Wang, Nature Photonics 2013, 7, 752.

[22] W. Wu, L. Wang, R. Yu, Y. Liu, S. H. Wei, J. Hone, Z. L. Wang, Adv Mater 2016, 28, 8463.

[23] C. Pan, S. Niu, Y. Ding, L. Dong, R. Yu, Y. Liu, G. Zhu, Z. L. Wang, Nano Lett 2012, 12, 3302; G. Michael, Y. Zhang, J. Nie, D. Zheng, G. Hu, R. Liu, M. Dan, L. Li, Y. Zhang, Nano Energy 2020, 76.

[24] S. C. Rai, K. Wang, Y. Ding, J. K. Marmon, M. Bhatt, Y. Zhang, W. Zhou, Z. L. Wang, ACS Nano 2015, 9, 6419; Q. Lai, L. Zhu, Y. Pang, L. Xu, J. Chen, Z. Ren, J. Luo, L. Wang, L. Chen, K. Han, P. Lin, D. Li, S. Lin, B. Chen, C. Pan, Z. L. Wang, ACS Nano 2018, 12, 10501.

[25] Y. Liu, S. Niu, Q. Yang, B. D. Klein, Y. S. Zhou, Z. L. Wang, Adv Mater 2014, 26, 7209.

[26] A. Sultana, P. Sadhukhan, M. M. Alam, S. Das, T. R. Middya, D. Mandal, ACS applied materials & interfaces 2018, 10, 4121.

[27] F. Cao, W. Tian, L. Meng, M. Wang, L. Li, Advanced Functional Materials 2019, 29, 1808415.

[28] F. Cao, W. Tian, M. Wang, H. Cao, L. Li, Advanced Functional Materials 2019, 29, 1901280.

[29] G. Hu, W. Guo, R. Yu, X. Yang, R. Zhou, C. Pan, Z. L. Wang, Nano Energy 2016, 23, 27; C. Wang, R. Bao, K. Zhao, T. Zhang, L. Dong, C. Pan, Nano Energy 2015, 14, 364; K. Zhang, M. Peng, W. Wu, J. Guo, G. Gao, Y. Liu, J. Kou, R. Wen, Y. Lei, A. Yu, Y. Zhang, J. Zhai, Z. L. Wang, Materials Horizons 2017, 4, 274.

[30] T. Y. Zhang, N. J. Guo, G. Li, X. F. Qian, Y. X. Zhao, Nano Energy 2016, 26, 50.

[31] E. Jia, D. Wei, P. Cui, J. Ji, H. Huang, H. Jiang, S. Dou, M. Li, C. Zhou, W. Wang, Adv Sci (Weinh) 2019, 6, 1900252.

[32] J. Ma, L. W. Wang, Nano Lett 2015, 15, 248.

[33] X. Xu, Z. Li, J. Wang, B. Lin, W. Ma, Y. Xia, M. R. Andersson, R. A. J. Janssen, E. Wang, Nano Energy 2018, 45, 368.

[34] B. Qi, J. Wang, Physical Chemistry Chemical Physics 2013, 15, 8972.

[35] C.-H. Chiang, C.-G. Wu, Nature Photonics 2016, 10, 196.

[36] J. H. Heo, S. H. Im, J. H. Noh, T. N. Mandal, C.-S. Lim, J. A. Chang, Y. H. Lee, H.-j. Kim, A. Sarkar, M. K. Nazeeruddin, Nature photonics 2013, 7, 486.

[37] H. D. Kim, H. Ohkita, Solar RRL 2017, 1, 1700027.

[38] H. Tan, A. Jain, O. Voznyy, X. Lan, F. P. Garcia de Arquer, J. Z. Fan, R. Quintero-Bermudez, M. Yuan, B. Zhang, Y. Zhao, F. Fan, P. Li, L. N. Quan, Y. Zhao, Z. H. Lu, Z. Yang, S. Hoogland, E. H. Sargent, Science 2017, 355, 722.

[39] J. Zhuang, P. Mao, Y. Luan, X. Yi, Z. Tu, Y. Zhang, Y. Yi, Y. Wei, N. Chen, T. Lin, F. Wang, C. Li, J. Wang, ACS Energy Letters 2019, 2913.

[40] C. C. Stoumpos, C. D. Malliakas, M. G. Kanatzidis, Inorg Chem 2013, 52, 9019.

[41] J. Li, L. Cai, J. Shang, Y. Yu, L. Zhang, Adv Mater 2016, 28, 4059.

[42] S. Y. Yang, J. Seidel, S. J. Byrnes, P. Shafer, C. H. Yang, M. D. Rossell, P. Yu, Y. H. Chu, J. F. Scott, J. W. Ager, 3rd, L. W. Martin, R. Ramesh, Nat Nanotechnol 2010, 5, 143.

[43] Y. Hu, Y. Pan, Z. Wang, T. Lin, Y. Gao, B. Luo, H. Hu, F. Fan, G. Liu, L. Wang, Nat Commun 2020, 11, 2129.

[44] N. Yaacobi-Gross, M. Soreni-Harari, M. Zimin, S. Kababya, A. Schmidt, N. Tessler, Nat Mater 2011, 10, 974.

[45] V. D. Mihailetchi, L. J. Koster, J. C. Hummelen, P. W. Blom, Phys Rev Lett 2004, 93, 216601.

[46] K. Kathan-Galipeau, P. Wu, Y. Li, L.-Q. Chen, A. Soukiassian, X. Xi, D. G. Schlom, D. A. Bonnell, ACS nano 2011, 5, 640.

[47] D. Taguchi, T. Shino, L. Zhang, J. Li, M. Weis, T. Manaka, M. Iwamoto, Applied physics express 2011, 4, 021602.

[48] S. J. Lee, H.-J. Jo, M. G. So, C. W. Sohn, J. S. Kim, I.-H. Bae, S. J. Lee, S. K. Noh, H. Choi, J.-Y. Leem, Journal of the Korean Physical Society 2015, 66, 667.

[49] J. Fu, Y. Hou, M. Zheng, M. Zhu, Journal of materials science 2018, 53, 7233.

[50] Z. Xiao, Y. Yuan, Y. Shao, Q. Wang, Q. Dong, C. Bi, P. Sharma, A. Gruverman, J. Huang, Nat Mater 2015, 14, 193.

[51] T. Choi, S. Lee, Y. J. Choi, V. Kiryukhin, S. W. Cheong, Science 2009, 324, 63.

[52] N. B. Zhitenev, A. Sidorenko, D. M. Tennant, R. A. Cirelli, Nat Nanotechnol 2007, 2, 237.

[53] C. W. Tang, Applied physics letters 1986, 48, 183.

Acknowledgments

The authors are thankful for the support from the University of Electronic Science and Technology of China (ZYGX2015-KYQD063). LL would like to thank the European Regional Development Fund (ERDF) for funding the Solar Photovoltaic Academic Research Consortium (SPARC II).

Author contributions

Y.Z., J.Z.W. and L.J.L. conceived the project. Y.Z. J.H.N. and designed the experiments. J.H.N. and M.J.D. carried out the experiments. Y.Z., J.H.N. and Y.M.Z. performed the theoretical calculations and analysis. All authors contributed to discussions and analyzed the results. J.H.N. wrote the manuscript and Y.Z., J.Z.W. and L.J.L. revised the manuscript.

Additional information

Supplementary information is available in the online version of the paper. Reprints and permissions information is available online. Correspondence and requests for materials should be addressed to Y.Z..

Competing interests

The authors declare no competing interests.

Figure caption

Figure 1 | (a) The spontaneous P(VDF-TrFE) doped n-i-p structured perovskite solar cell. (b) The polarization process via an external electric field. (c) The polarized P(VDF-TrFE) induced electronic field affects transport behavior of electrons and holes. (d) A schematic diagram of electric field induced by the P(VDF-TrFE) driving separation and transportation of the electrons and holes. (e) The molecule structures of perovskite films. (f) The molecule structures of P(VDF-TrFE) polymers.

Figure 2 | (a) SEM image of untreated perovskites film. (b) SEM image of P(VDF-TrFE) doped perovskites film. (c) Size scale of untreated perovskites film and P(VDF-TrFE) doped perovskites film. (d) PL spectra of P(VDF-TrFE) doped perovskites film in different concentrations. (e) XRD of the perovskite film doped with various concentrations of P(VDF-TrFE) polymer. (f) power conversion efficiency of perovskite solar cells with different concentrations of P(VDF-TrFE) polymer.

Figure 3 | power conversion efficiency of perovskite solar cells with different poling time in the condition of positive polarization (a) and negative polarization (b).

Figure 4 | The schematic diagram of energy bands for p-i-n (SnO2-$(FAPbI3)_{1-x}(MAPbBr_{3-y}Cl_y)_x$ -SpiroMeOTAD) solar cells under the conditions of spontaneous polarization (a), positive poling (b) and negative poling (c).

Figure 5 | The surface potential patterns at the interface of P(VDF-TrFE)/perovskite with the P(VDF-TrFE) concentration of 0 mg (a), 1 mg (b), 2 mg (c), 4 mg (d). (e) The surface potential distribution along the white lines in (a) and (c). (f) The surface potential statistical distribution in (a) and (c).

Table caption

Table 1 | Photovoltaic performance of the solar cells based on doping P(VDF-TrFE) materials

Table 2 | Photovoltaic performance of the solar cells based on positive pre-poling.

Table 3 | Photovoltaic performance of the solar cells based on negative pre-poling.

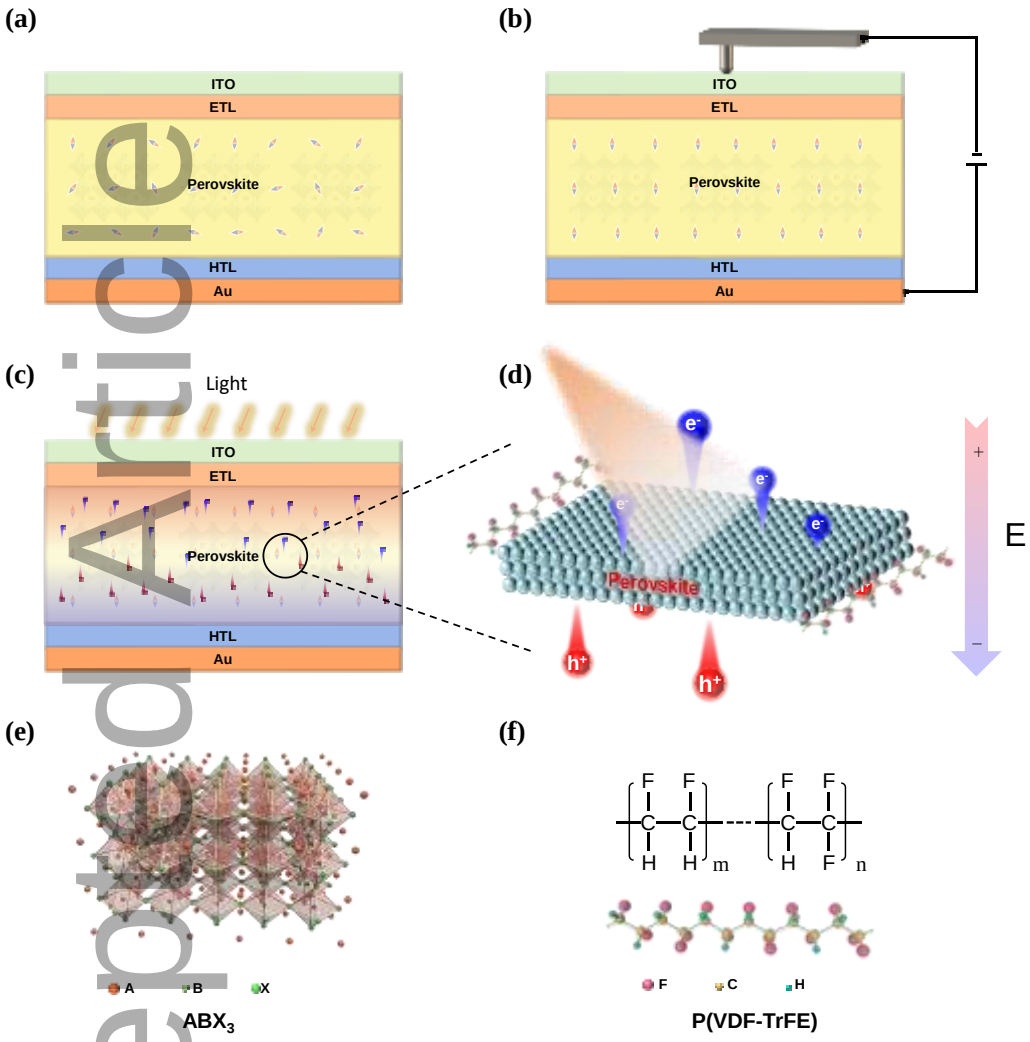

Figure 1

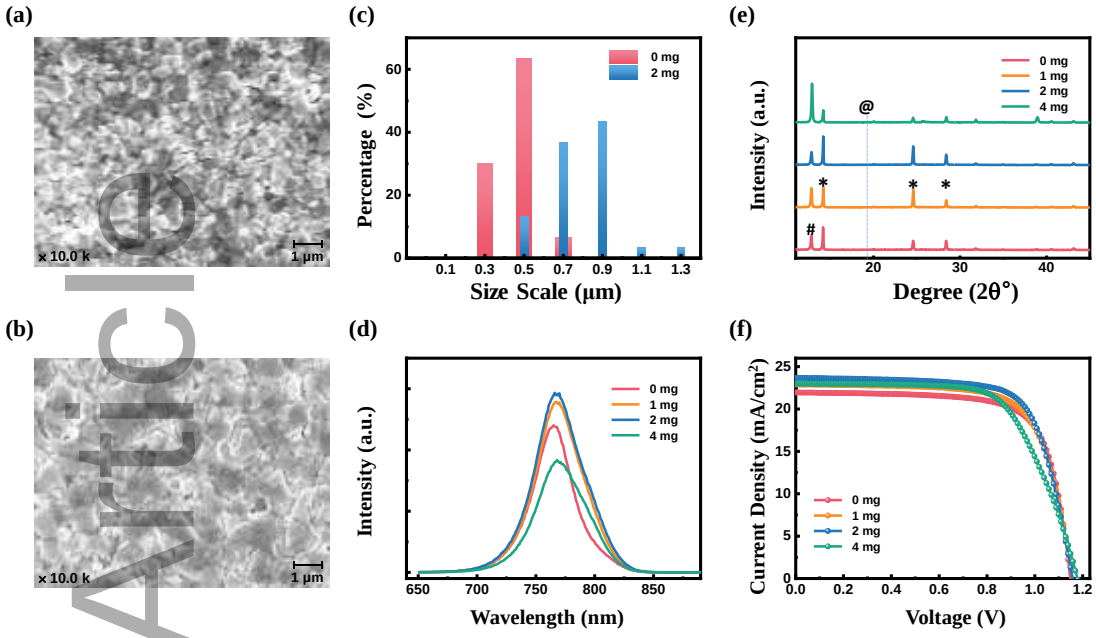

Figure 2

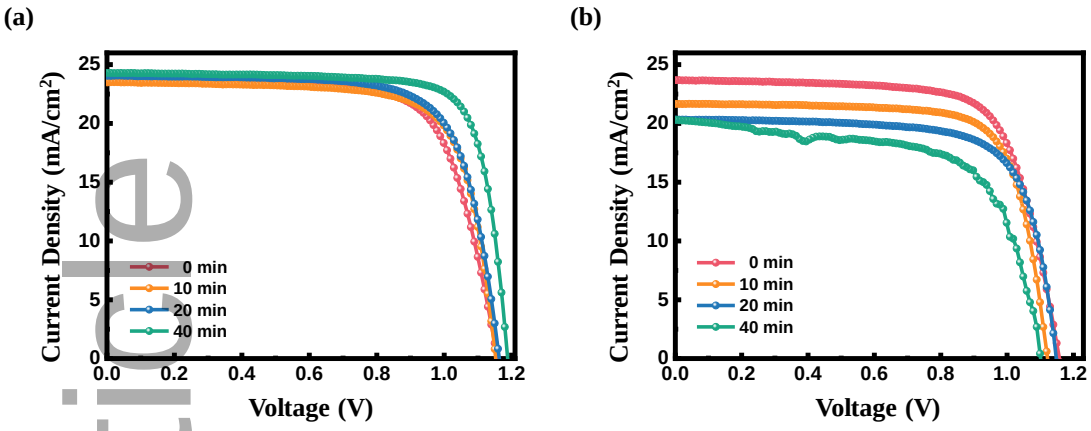

Figure 3

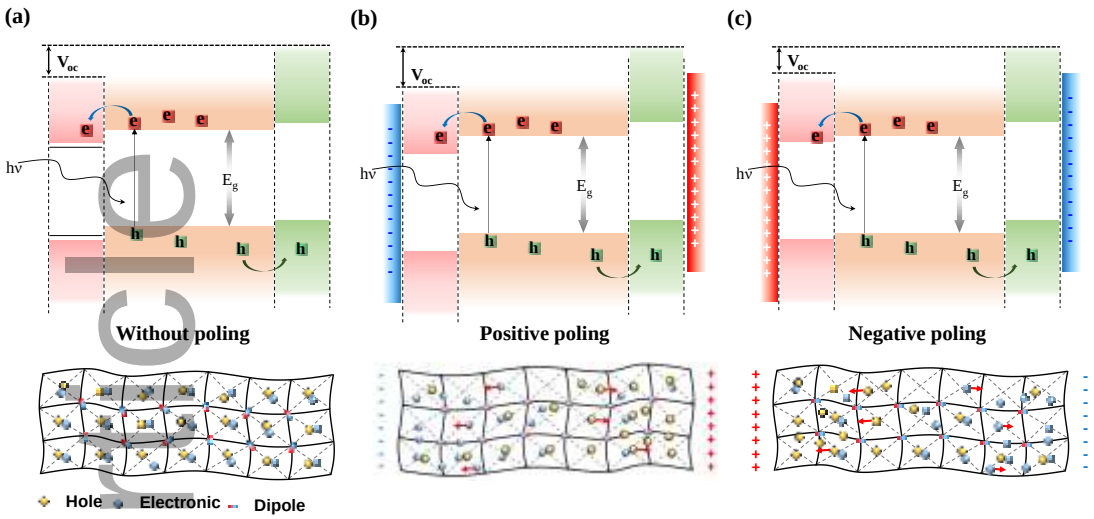

Figure 4

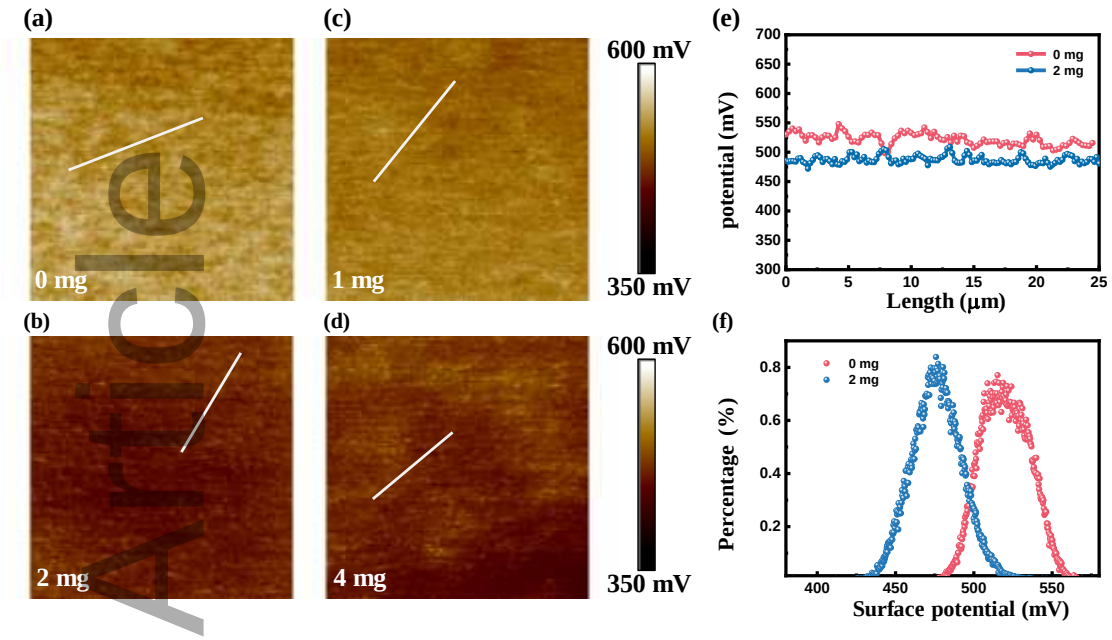

Figure 5

Table 1. Photovoltaic performance of the solar cells based on doping P(VDF-TrFE) materials.

PVDF-TrFE [mg]	PCE [%]	J_{sc} [mA/cm^2]	FF [%]	V_{oc} [V]
0	18.3	21.9	72.8	1.14
1	19.2	22.9	72.9	1.16
2	20.3	23.6	72.1	1.16
4	18.8	22.9	69.0	1.18

Table 2. Photovoltaic performance of the solar cells based on positive pre-poling.

Poling time [min]	PCE [%]	J_{sc} [mA/cm^2]	FF [%]	V_{oc} [V]
0	20.3	23.6	72.1	1.17
10	20.8	23.4	76.0	1.17
20	21.6	24.0	76.1	1.18
40	22.1	24.2	78.0	1.18

Table 3. Photovoltaic performance of the solar cells based on negative pre-poling.

Poling time [min]	PCE [%]	J_{sc} [mA/cm^2]	FF [%]	V_{oc} [V]
0	20.5	23.5	77.0	1.13
10	18.1	21.7	75.0	1.12
20	16.9	20.3	72.7	1.14
40	14.3	20.2	64.0	1.09

Piezo-phototronic Effect Enhanced Perovskite Solar Cell Based on P(VDF-TrFE)

Jiaheng Nie [1,2], Yaming Zhang[1], Minjiang Dan[1], Jizheng Wang [2,*], Lijie Li [3,*], and Yan Zhang[1,*]

[1] *School of Physics, University of Electronic Science and Technology of China, Chengdu 610054, China*

[2] *Chinese Acad Sci, Inst Chem, Beijing Natl Lab Mol Sci, CAS Key Lab Organ Solids, Beijing 100190, China.*

[3] *College of Engineering, Swansea University, Swansea, SA1 8EN, UK*

[*] To whom correspondence should be addressed, E-mail: zhangyan@uestc.edu.cn, L.Li@swansea.ac.uk and jizheng@iccas.ac.cn

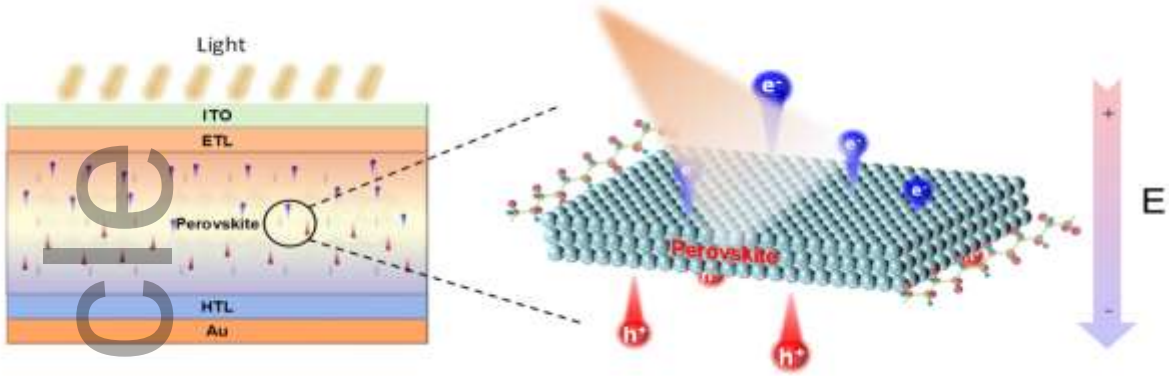

A simple poling process that simultaneously modulates the built-in field and interface barriers of the perovskite solar cell devices has been conducted for the perovskite material doped by P(VDF-TrFE). It has been unveiled that the newly developed solar cell devices have achieved a high power conversion effectivity of 22.1%, which is attributed to the piezophototronic effect that can effectively enhance the performance of perovskite solar cell.